A comb laser-driven DWDM silicon photonic transmitter based on microring modulators

Chin-Hui Chen,[1,*] **M. Ashkan Seyedi,**[1] **Marco Fiorentino,**[1] **Daniil Livshits,**[2] **Alexey Gubenko,**[2] **Sergey Mikhrin,**[2] **Vladimir Mikhrin,**[2] **and Raymond G. Beausoleil**[1]

[1]*HP Labs, Hewlett-Packard Company, Palo Alto, CA, USA*
[2]*Innolume GmbH, Dortmund, Germany*
[*]*chin-hui.chen@hp.com*

Abstract: We demonstrate concurrent multi-channel transmission at 10 Gbps per channel of a DWDM silicon photonic transmitter. The DWDM transmitter is based on a single quantum dot comb laser and an array of microring resonator-based modulators. The resonant wavelengths of microrings are thermally tuned to align with the wavelengths provided by the comb laser. No obvious crosstalk is observed at 240 GHz channel spacing.

References and links

1. Cisco System Inc., "Cisco Global Cloud Index: Forecast and Methodology, 2013–2018," (2014).
2. D. A. B. Miller, "Optical interconnects to electronic chips," Applied Optics **49**(25), F59–F70 (2010).
3. R. G. Beausoleil, "Large-scale integrated photonics for high-performance interconnects," J. Emerg. Technol. Comput. Syst., ACM **7**(2), 6:1–6:54 (2011).
4. A. P. Knights, E. Huante-Ceron, J. Ackert, D. Logan, G. Wojcik, F. Zhang, A. Gubenko, and S. Mikhrin, "Comb-laser driven WDM for short reach silicon photonic based optical interconnection," IEEE 9th International Conference on Group IV Photonics (GFP), 210–212 (2012).
5. X. Zheng, E. Chang, I. Shubin, G. Li, Y. Luo, J. Yao, H. Thacker, J.-H. Lee, J. Lexau, F. Liu, P. Amberg, K. Raj, R. Ho, J. E. Cunningham, and A. V. Krishnamoorthy, "A 33 mW 100 Gbps CMOS Silicon Photonic WDM Transmitter Using Off-Chip Laser Sources," Optical Fiber Communication Conference (OFC) **PDP5C.9** (2013).
6. D. Livshits, D. Yin, A. Gubenko, I. Krestnikov, S. Mikhrin, A. Kovsh and G. Wojcik, "Cost-effective WDM optical interconnects enabled by quantum dot comb lasers," Proc. SPIE **7607**, Optoelectronic Interconnects and Component Integration IX, 76070W (2010).
7. Q. Xu, B. Schmidt, J. Shakya, and M. Lipson, "Cascaded silicon micro-ring modulators for WDM optical interconnection," Opt. Express **14**(20), 9431–9435 (2006).
8. S. Manipatruni, L. Chen, and M. Lipson, "Ultra high bandwidth WDM using silicon microring modulators," Opt. Express **18**(16), 16858–16867 (2010).
9. Y. Liu, R. Ding, Q. Li, Z. Xuan, Y. Li, Y. Yang, A. E.-J. Lim, P. G.-Q. Lo, K. Bergman, T. Baehr-Jones, and M. Hochberg, "Ultra-compact 320 Gb/s and 160 Gb/s WDM transmitters based on silicon microrings," Optical Fiber Communication Conference (OFC) **Th4G.6** (2014).
10. T. Baba, S. Akiyama, M. Imai, N. Hirayama, H. Takahashi, Y. Noguchi, T. Horikawa, and T. Usuki, "50-Gb/s ring-resonator-based silicon modulator," Opt. Express **21**, 11869-11876 (2013).
11. C. Li, R. Bai, A. Shafik, E.Z. Tabasy, G. Tang, C. Ma, C.-H. Chen, Z. Peng, M. Fiorentino, P. Chiang, and S. Palermo, "A ring-resonator-based silicon photonics transceiver with bias-based wavelength stabilization and adaptive-power-sensitivity receiver," IEEE Solid-State Circuits Conference Digest of Technical Papers (ISSCC), 124–125 (2013).

12. C. Li, R. Bai, A. Shafik, E.Z. Tabasy, G. Tang, C. Ma, C.-H. Chen, Z. Peng, M. Fiorentino, P. Chiang, and S. Palermo, "Silicon Photonic Transceiver Circuits With Microring Resonator Bias-Based Wavelength Stabilization in 65 nm CMOS," IEEE Journal of Solid-State Circuits, **49**(6), 1419–1436 (2014).
13. C.-H. Chen, C. Li, A. Shafik, M. Fiorentino, P. Chiang, S. Palermo, and R. Beausoleil, "A WDM silicon photonic transmitter based on carrier-injection microring modulators," IEEE Optical Interconnects Conference, **WC3**, 121–122 (2014).
14. C.-H. Chen, C. Li, R. Bai, K. Yu, J.-M. Fedeli, S. Meassoudene, M. Fournier, S. Menezo, P. Chiang, S. Palermo, M. Fiorentino, and R. Beausoleil, "DWDM Silicon Photonic Transceivers for Optical Interconnect," IEEE Optical Interconnects Conference, **TuD1** (invited), 52–53 (2015).
15. K. Yu, C.-H. Chen, C. Li, H. Li, A. Titriku, B. Wang, A. Shafik, Z. Wang, M. Fiorentino, P. Y. Chiang, and S. Palermo, "25 Gb/s hybrid-integrated silicon photonic receiver with microring wavelength stabilization," Optical Fiber Communication Conference (OFC) **W3A.6** (2015).
16. C.-H. Chen, T.-C. Huang, D. Livshits, A. Gubenko, S. Mikhrin, V. Mikhrin, M. Fiorentino, and R. Beausoleil, "A comb laser-driven DWDM silicon photonic transmitter with microring modulator for optical interconnect," Conference on Lasers and Electro-Optics (CLEO) **STu4F.1** (2015).
17. G. L. Wojcik, D. Yin, A. R. Kovsh, A. E. Gubenko, I. L. Krestnikov, S. S. Mikhrin, D. A. Livshits, D. A. Fattal, M. Fiorentino, and R. G. Beausoleil, "A single comb laser source for short reach WDM interconnects," Proc. SPIE 7230, Novel In-Plane Semiconductor Lasers VIII, 72300M (2009).
18. Q. Xu, S. Manipatruni, B. Schmidt, J. Shakya, and M. Lipson, "12.5 Gbit/s carrier-injection-based silicon micro-ring silicon modulators," Opt. Express **15**(2), 430–436 (2007).
19. M. Georgas, J. Leu, B. Moss, C. Sun, and V. Stojanovic, "Addressing link-level design tradeoffs for integrated photonic interconnects," Proceedings of IEEE Custom Integrated Circuits Conference (CICC), 1–8 (2011).
20. D. Livshits, A. Gubenko, S. Mikhrin, V. Mikhrin, C.-H. Chen, M. Fiorentino, and R. Beausoleil, "High efficiency diode comb-laser for DWDM optical interconnects," IEEE Optical Interconnects Conference, 83–84 (2014).
21. K. Padmaraju, X. Zhu, L. Chen, M. Lipson, and K. Bergman, "Intermodulation Crosstalk Characteristics of WDM silicon microring modulators," IEEE Photonics Technology Letters **26**(14), 1478–1481 (2014).

1. Introduction

The persistent pursuit of higher performance computing and faster cloud connectivity within stringent power constraints has expedited the computational parallelism to grow exponentially. One recent report [1] suggests that the global datacenter traffic will triple from 2013 to 2018 to reach 8.6 ZB annually, and three-fourths of the traffic remains within the datacenter. The massive amount of the data movement for machine-to-machine traffic demands innovations in short-reach interconnects to provide denser connectivity with high bandwidth, low latency, and high energy efficiency in a cost-effective manner, which can not be delivered by incremental improvements of existing technologies. Optical interconnects are emerging as a viable solution over copper wires for board-to-board data communication. As the strong demand for bandwidth continues to increase, advanced optical interconnects are progressively penetrating into shorter distances inside the chassis and moving towards the chip-to-chip interconnects for processors and switches [2, 3].

Silicon photonics is considered an economical candidate for optical interconnects by taking advantages of the existing CMOS-VLSI infrastructure to offer unprecedented bandwidth scalability using dense wavelength division multiplexing (DWDM). A promising approach pairs innovations in quantum dot (QD) multi-wavelength lasers with silicon photonic microring resonators to fulfill aforementioned needs and leads to low-cost and scalable DWDM solutions [4]. The multi-wavelength DWDM spectrum can be generated by either an array of single-wavelength lasers [5] or a single comb laser. However, temperature control, wavelength tracking, and complicated packaging make the laser array impractical at a large scale. On the other hand, a single diode comb laser based on QDs provides multiple narrow-spectrum and low-noise laser tones, each corresponding to a longitudinal cavity mode [6]. The QD comb laser enables a much simpler and more compact interface design, and therefore renders nanophotonic interconnects with lower power consumption when compared to an equivalent design with multiple discrete lasers and components.

Cascaded microring modulators are one of the promising methods to create multiple inde-

pendently modulated data streams at different wavelengths for short-reach DWDM link. Silicon microring resonators are not only compact and consume low power, but also do not require an additional multiplexer compared to conventional broadband modulators. Significant progress has been made in this area [5, 7–9], however, previous demonstrations are often characterized using single-wavelength tunable lasers one channel at a time.

We choose carrier-injection silicon modulator for developing our future photonic systems because of many merits such as high extinction ratio, low optical insertion loss, and low driving voltage required. If taking into account the CMOS driver design for microring modulator, low driving voltage can enable the use of most advanced CMOS technologies that is beneficial for optimizing the energy efficiency. In terms of CMOS receiver design, high extinction ratio and low insertion loss can relax the sensitivity requirement imposed to the receiver that also helps to improve the energy efficiency. On the other hand, the lower data rate of the carrier-injection silicon modulator can be alleviated by using advanced modulation schemes such as pulse-amplitude modulation (PAM) or multiplexing methods such as WDM to increase the overall data throughput. By improving the driving techniques and feed-forward equalizer (FFE) design, a 50 Gbps carrier-injection ring modulator has been published in recent literatures [10]. We do not simply use carrier-injection modulator as a means for system demonstration, but also believe that it will be beneficial in terms of photonic system design, since data rate is only one single factor to consider.

Over the years we have developed DWDM CMOS photonic transceivers that are hybridly integrated via either wirebonding or flip-chip bonding [11–15]. The CMOS die is implemented at 65 nm technology node with multi-project shuttle runs at TSMC, and the integrated photonic transceivers based on carrier-injection microring modulators, drop filters, and germanium photodiodes are implemented with dedicated wafer batches at CEA-Leti, an external foundry specialized in CMOS-compatible silicon photonics platform. The CMOS drivers serve two main purposes: 1) feedback control and stabilizing the wavelength by both thermal and bias tuning, and 2) providing pre-emphasized driving signals to compensate for the low signal bandwidth of the carrier-injection modulator in order to achieve higher data rates. In terms of the receiver design, we also use microring resonator as the DWDM optical drop filter. Thanks to the high extinction ratio and low insertion loss of injection-type of silicon modulator, the CMOS receiver can be designed for higher bandwidth with similar or less total power consumption compared with the CMOS receiver for depletion-type of silicon modulator because of relaxed signal amplification requirements.

We have previously demonstrated a comb laser-driven microring modulator-based transmitter for DWDM applications [16]. Similar eye quality as measured by tunable lasers has demonstrated its potential for error-free transmission at high speeds. The comb spectrum, however, was filtered at the input and only one channel was modulated. In this paper, we demonstrate simultaneous multi-channel transmission of a DWDM silicon photonic transmitter with an array of microring modulators driven by an unfiltered QD comb laser. It is an important step forward to characterize crosstalks and signal integrity. Two microrings are optically excited and modulated concurrently at 10 Gbps with independent data streams. No significant signal degradation due to wavelength crosstalk is observed at 240 GHz channel spacing, indicating the possibility of further signal bandwidth scaling.

2. Quantum-Dot Comb Laser

QD lasers draw particular attention in optical communication systems. The three-dimensional quantum confinement of the electrons and holes in a QD results in discrete density of states. Besides an increase in material gain and a reduction in threshold current density compared to bulk materials or quantum well structures, QD lasers also have a greater resilience to temperature

changes owing to the absence of higher energy states that can be thermally populated. Broadband emission requirements for WDM applications benefit from the inhomogeneous broadening of the gain spectrum due to the size dispersion of QDs.

Multi-wavelength emission can be generated by a single Fabry-Perot (FP) comb laser diode based on InAs/GaAs QDs [17]. Figure 1(a) shows LIV curves of a comb laser used in this work measured after a fiber-coupled isolator. The temperature range from 15 °C to 55 °C is limited by the temperature controller used in the measurement. Wall-plug efficiencies (WPE) as shown in Fig. 1(b) are around 10% between 25 °C and 45 °C. The optical spectrum in Fig. 1(c) shows ten 80 GHz-spaced comb lines with output power level of 1 to 2 mW. The free spectral range (FSR) of the optical comb matches to the FP longitudinal mode spacing corresponding to the cavity length.

The 80 GHz is a result of optimization of FP comb laser, particularly in terms of WPE. WPE is not a monotonic function of the channel spacing, which is proportional to reciprocal laser cavity length. If the cavity is too long, WPE is low due to the internal optical loss. If the cavity is too short, WPE is low due to the carrier loss (low internal quantum efficiency). In QD Fabry-Perot lasers a cavity length of 500-1000 μm (about 40-80 GHz channel spacing) seems to be optimal. The exact values depend on the concrete design of the epi-structure and the device construction. Further increasing of the channel spacing decreases both WPE and maximal achievable power. Further increasing of the channel spacing decreases both WPE and maximal achievable power. Nevertheless, one can try to break this trade-off. One approach is to decrease cavity length and to compensate the excess radiative loss by proper HR coating of front mirror. Another approach is based on the harmonic mode-locking. Third approach is monolithic integration of short-cavity distributed Bragg reflector (DBR) laser with the amplifier section. We are pursuing in all these directions.

We observe a low threshold current of 8 mA at 25 °C, and the threshold current increases to 15 mA at 55 °C. Reduced amplified spontaneous emission (ASE) exhibited in QD-based material helps to ensure low spontaneous fluctuation in the gain and the refractive index, which is one of the major factors of timing jitter at high-speed operation. Relative intensity noise (RIN) of -120 to -145 dB/Hz is measured from 10 MHz to 10 GHz.
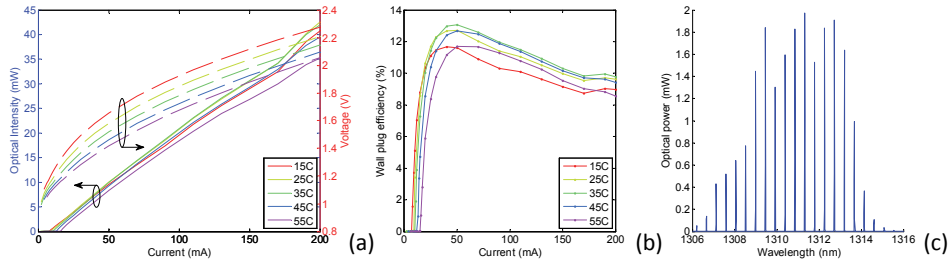

Fig. 1. Comb laser characteristics: (a) LIV curves, (b) wall-plug efficiency at various operating temperatures, and (c) optical spectrum at 25 °C and bias current of 150 mA.

3. Multi-Channel Microring Resonator-Based Modulators

We have fabricated a five-channel photonic integrated circuit [13] on 200-mm silicon-on-insulator (SOI) wafers using CMOS compatible processes as shown in Fig. 2(a). The device configuration and pad layout are designed to be compatible with flip-chip bonding to a CMOS transceiver die [14]. The rib waveguide is 250 nm in height and 450 nm in width, and the slab

thickness is 50 nm. The microring resonators with radii around 5 μm as shown in Fig. 2(b) and (c) are designed to provide five resonant wavelengths with 160 GHz channel spacing, which skips every other channel in the comb of wavelength to minimize optical crosstalk in this demonstration. The FSR of the microring resonator is measured to be 11.4 nm, which offers the ability to allocate up to 24 channels at 80 GHz spacing near 1.31 μm wavelengths.
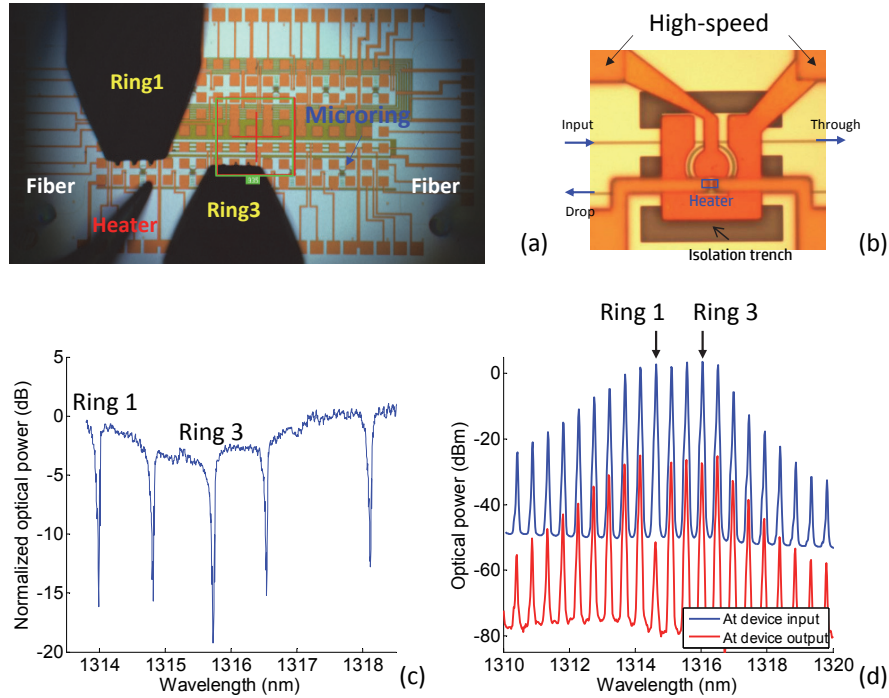

Fig. 2. (a) Microscope image of a 5-channel photonic transmitter. High-speed modulation are applied to Ring1 and Ring3 simultaneously. A common ground pad (outside the scope view) is connected as the other terminal of heater. (b) Microscope image of a microring resonator with 5 μm radius. (c) Optical spectrum of the five cascaded microring resonators without tuning. (d) Optical comb spectra of the amplified comb source at the device input (blue) and at the device output (red) with Ring1 aligned to one channel grid. The laser is biased at 165 mA, 25 °C.

There are several common mechanisms used in silicon modulators to vary carrier concentration such as carrier depletion in a PN diode, carrier injection in a PIN diode, and carrier accumulation in a metal-oxide-semiconductor (MOS) capacitor. Among these types, carrier-injection-based devices under forward bias can provide large changes of refractive index and high modulation depths. Free electrons and holes are injected into the intrinsic waveguide region to overlap with the optical mode, thus minimizing optical loss. Due to inherently slow carrier lifetime, however, pre-emphasized driving signals are required for high-speed operation [10,18]. It has been analyzed that if the Nyquist frequency of the data communication over the optical interconnects exceeds twice the clock frequency of the underlying silicon, significant power penalties become inevitable due to signal serialization and deserialization (SerDes) [19], so we choose a moderate data rate and use carrier-injection modulators as the key ingredients to pursue the optimal energy-efficiencies for optical interconnects.

Due to process variations, the as-built resonant wavelengths of the microring resonators slightly deviated from the design values. We actively align the resonance to match the comb source by thermal tuning via integrated doped-silicon heaters next to the microring waveguides. The thermal tuning efficiency is characterized to be 23 µW/GHz. There is also an integrated Ge waveguide photodiode at the drop port of the microring. It can be used along with the on-chip thermal tuner for active wavelength stabilization when combined with CMOS tuning circuitry [15]. Complementary bias-tuning has also been demonstrated to tune towards shorter wavelength with lower power consumption [11]. The quality factors of the microrings are more than 12,000, and the extinction ratios are 10–15 dB.

4. Measurement and Discussion

We have previously demonstrated 10 Gbps transmission of the microring modulator using a tunable laser at all five channels [13], and Fig. 3(a) shows one of the eye diagrams driven by PRBS31 pre-emphasized signals with 3 dBm optical power at the fiber input. Currently the high input power is required due to non-optimized grating couplers with 10 dB coupling loss to a single mode fiber (SMF), which are implemented by a single etch step (versus double-etched) to save one photo mask layer for economical prototyping. We then substitute the tunable laser with a spectrally filtered comb laser mode. We connect the comb laser to a QD-based semiconductor optical amplifier (SOA) and an optical filter before being coupled to the photonic chip. The comb spectral shape is maintained after amplification. The optical filter results in more than 30 dB side mode suppression but has a high insertion loss of 10 dB, and thus an SOA is needed to maintain the same optical power at the input. Figure 3(b) shows the eye diagram of a single microring modulator driven by the comb laser biased at 150 mA, 25 °C with similar eye quality compared to Fig. 3(a). The noise contribution from the comb laser and the SOA is considered to be minimal.
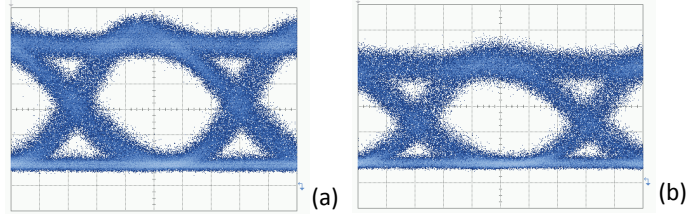

Fig. 3. Measured eye diagrams at 10 Gbps for a single microring modulator driven by (a) a tunable laser (29 µW/div) and (b) a spectrally filtered mode from a comb laser (37 µW/div).

Next, we study DWDM transmission using the five-channel device driven by an unfiltered comb laser. The measurement setup is shown in Fig. 4. We bias the comb laser at 165 mA in order to match to the resonant wavelengths of the microrings. Figure 2(d) shows a uniform comb spectrum of wavelength between 1313–1317 nm with 80 GHz spacing, and the power levels are in the range of 1.5 to 3.5 dBm after amplification at the fiber input. A high insertion loss (-24 dB) of the photonic die is attributed to the non-optimized grating coupler as well as the long bus waveguide. Using a comb laser with higher WPE [20] and improving fiber coupling should eliminate the use of SOA in the future.

Two microrings, namely Ring1 and Ring3, are modulated simultaneously by two separate pulse pattern generators (PPG). The pre-emphasized electrical driving signal is generated by combining the *DATA* and $\overline{DATA}$ output of a PRBS7 source with a tuneable delay line. Each
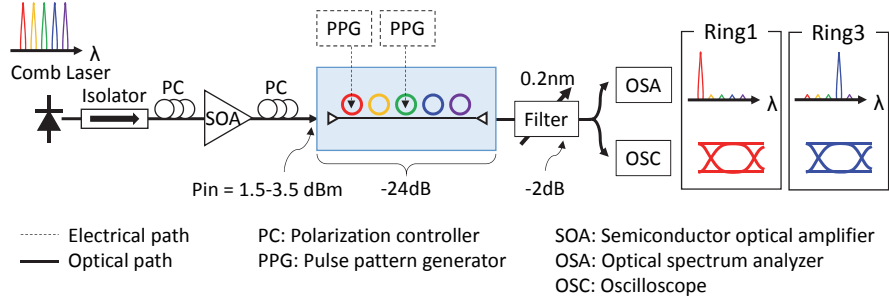
Fig. 4. Schematics of DWDM photonic transmitter measurement setup.

output of the two PRBS sources can be configured with a peak to peak voltage (V_{pp}) and a DC bias (V_{dc}) to create the pre-emphasis. The driving schemes for both microrings are shown in Table 1. These values are individually controlled for optimizing the output eye and are within the voltage range of a CMOS cascode driver [11].

The spacing between the two resonance of Ring1 and Ring3 is designed to be 320 GHz. Due to physical space limitations in our probe station, only the thermal heater of Ring1 is connected. To accommodate fabrication variation, we red-shifted Ring1 to align with the next comb line and thus measured the two channels at 240 GHz spacing. Figure 2(c) also shows the optical output spectrum with Ring1 aligned to one comb-line resulting in 20 dB suppression. The modulated light at individual channel are spectrally selected at the output by a tunable filter consisting of a fiber Bragg grating (FBG) and an optical circulator. The FBG-based filter has a 0.2 nm pass-band and 2 dB insertion loss.

Table 1. Parameters for pre-emphasis signals

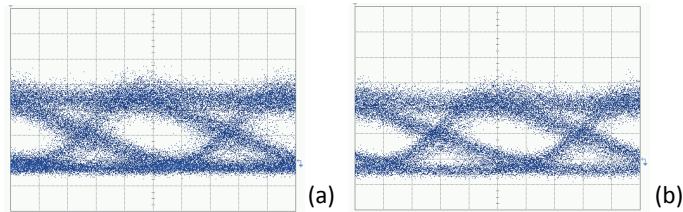|	Ring1		Ring3	
	DATA	$\overline{DATA}$	DATA	$\overline{DATA}$
V_{pp} (V)	1.7	1.6	1.5	1.34
V_{dc} (V)	0.86	0	0.91	0

Fig. 5. Measured eye diagrams at 10 Gbps of simultaneously modulated channels at (a) Ring1 (2 μW/div) and (b) Ring3 (2 μW/div) of the five-channel transmitter.

Figure 5 shows the eye diagrams of Ring1 and Ring3 that are both independently modulated at 10 Gbps at the same time. The high insertion loss of multi-channel device is mainly attributed to the non-optimized grating couplers. The waveguide length is 3 mm in multi-channel structure, which also introduces extra loss compared with the single ring structure. The received optical power is therefore very close to the limit of the detection sensitivity of the oscilloscope. Moving forward, we believe that by using a double-etched grating coupler (2-3 dB loss) provided in Letis PDK we can improve the fiber-to-fiber loss from the current 24 dB to be 8-10 dB. This also allows us to eliminate the use of SOA at the input to further reduce power consumption of the system and remove the noise contribution from SOA. It has been reported that the crosstalk is negligible with spacing down to 100 GHz [21] for a typical silicon microring modulator operated at 10 Gbps. In this demonstration, we believe the wide channel separation of 240 GHz ensures low optical intermodulation crosstalk, and the physical distance (600 μm) between the two microrings eliminates the electrical RF crosstalk and thermal crosstalk. We will perform bit-error rate study to quantify the power penalty due to the crosstalk effects and further study the minimal channel spacing in the proposed system.

5. Conclusion

We choose the carrier-injection silicon modulator for our future photonic systems because of its high extinction ratio, low optical insertion loss, and low driving voltage required. It has merits for both transmitter and receiver designs for an energy-efficient nanophotonic system. We have developed DWDM CMOS photonic transceivers that are hybridly integrated via either wire-bonding or flip-chip bonding. The CMOS circuits provide active wavelength stabilization and signal pre-emphasis to achieve high data rates. We have demonstrated a DWDM photonic transmitter with concurrent multi-channel transmission at 10 Gbps based on a single QD comb laser and cascaded microring modulators. The resonant wavelengths of two microrings are aligned to the wavelengths provided by the comb laser through thermal tuning to be 240 GHz apart. We expect to eliminate the use of SOA by improving the comb laser and the fiber coupling. The 5-channel photonic transceiver implemented at a dedicated wafer-scale CMOS-compatible foundry process can be flip-chip bonded with a CMOS die to offer 100 Gbps bi-directional throughput. This represents an important step towards an ultra-compact and energy-efficient DWDM CMOS photonic interconnects.